FEBS 17374 FEBS Letters 391 (1996) 323–329

Mitochondrial ATP synthase F_1-β-subunit is a calcium-binding protein

Michael J. Hubbard*, Nicola J. McHugh

Department of Biochemistry, University of Otago, P.O. Box 56, Dunedin, New Zealand

Received 10 May 1996; revised version received 25 June 1996

Abstract Mitochondrial ATP synthase is responsive to changes in cytosolic calcium concentration, but the regulatory mechanisms are unclear. Here we identified a major 52 kDa calcium-binding protein in rat enamel cells as the mitochondrial ATP synthase F_1-β-subunit. The F_1-β-subunit behaved as a low affinity and moderate capacity calcium-binding protein during comparative ^{45}Ca overlay analyses. Equivalent behavior was shown by the F_1-β-subunit from rat liver mitochondria, but not by the homologous F_1-α-subunit, supporting the specificity of calcium binding. Evidence that the catalytic F_1-β-subunit binds calcium specifically introduces new mechanistic possibilities for regulating ATP synthase, and thereby coordinating ATP production with demand for ATP-fuelled calcium pump activity.

Key words: Calcium; ATP synthase; Mitochondria; Calcium-binding protein; Enamel cell; Methionine sulfoxide

1. Introduction

Mitochondria play a crucial role in intracellular calcium homeostasis, producing ATP to fuel the ATPases that pump calcium out of the cell or into organellar calcium stores such as the endoplasmic reticulum. Additionally, mitochondria are thought to buffer elevations of cytosolic calcium during both normal calcium signalling events and atypical calcium burdens (e.g. associated with biomineralization, disease and cell injury) [1–4].

Changes in cytosolic free calcium concentration are relayed to the mitochondrial matrix, enabling mitochondrial ATP production to respond to the varying ATP demands of intracellular calcium homeostasis [2,5–7]. Consistent with this scenario, several components of the ATP-producing machinery appear to be calcium-regulated. In the mitochondrial matrix, three NAD-linked dehydrogenases from the citric acid cycle are regulated either directly by calcium binding (isocitrate- and α-oxoglutarate dehydrogenases) or indirectly by calcium-dependent phosphorylation (pyruvate dehydrogenase). Activation of these dehydrogenases occurs at physiologically relevant (low micromolar) calcium concentrations [7]. The FAD-linked glycerol-3-phosphate dehydrogenase, located in the mitochondrial inner membrane where it contributes to the glycerol phosphate shuttle, is directly regulated by micromolar calcium. High affinity (EF hand) calcium-binding sites were identified in this protein recently [8]. ATP synthase (F_1F_o-ATPase or H^+-ATPase [9,10]), also situated in the mitochondrial inner membrane, appears sensitive to physiological levels of calcium [2,6,7,11]. One proposed mechanism involves a mitochondrial 6.5 kDa inhibitor protein, termed CaBI, that binds calcium with micromolar affinity and reversibly inhibits ATP synthase in a calcium-dependent manner in vitro [12,13]. However with added CaBI, elevated (low micromolar) calcium inhibits ATP synthase [13] rather than activating it as expected from the above scenario. Finally, a component of ATP synthase itself (i.e. the 8 kDa c-subunit of the F_o-complex from chloroplast and bacteria) was recently identified as a calcium-binding protein, and proposed to be involved in calcium gating of the F_o proton channel [14]. While calcium-dependent regulatory mechanisms have been identified both in the metabolic cycles that fuel ATP production and in the final catalytic complex, it remains unclear which of these have functional importance in vivo and how they interact with other controls (e.g. substrate variations).

Enamel cells handle large amounts of calcium when producing dental enamel, the most highly calcified (60% calcium by mass) tissue. We have commenced a biochemical investigation of enamel cell calcium homeostasis, anticipating that knowledge of how these cells handle bulk calcium will benefit understanding of calciotoxicity avoidance and of the associated links between calcium dishomeostasis, cell death and disease [15,16]. Enamel cells were found to contain a general high abundance of calcium-binding proteins, particularly during the postsecretory stage (termed maturation) when a major transcellular flux of calcium leads to enamel hypermineralization. Biochemical characterization of enamel cell calcium-binding proteins has been informative, providing novel support for the existence of $calbindin_{28kDa}$ target ligands [15,17] and unexpectedly pointing to an organellar- rather than cytosolic route for transcellular calcium transport [16]. Many major calcium-binding proteins in enamel cells remain to be identified.

This study addressed an enamel cell calcium-binding protein we recognized as having a possible role in transcellular calcium transport, given its high abundance and up-regulation during enamel maturation. Identification of this protein as the catalytic β-subunit of the F_1-complex (subunit composition $\alpha_3\beta_3\gamma\delta\varepsilon$) from mitochondrial ATP synthase, referred to here as the F_1-β-subunit, introduces a new potential mechanism for the calcium-dependent regulation of ATP synthesis.

2. Materials and methods

2.1. Tissue isolation and extracts

This study used Wistar-derived rats exposed to a 12-h fluorescent light cycle and sustained with unlimited access to a standard pellet chow and tap water.

Enamel epithelium was rapidly microdissected from mandibular first molars at differentiation, secretion and maturation phases (1-, 5- and 10-day-old pups, respectively), and micro-volume homogenates

*Corresponding author. Fax: (64) (3) 479 7866.
E-mail: mother@otago.ac.nz

Abbreviations: F_1-β-subunit, β-subunit of the F_1-complex from mitochondrial ATP synthase; MALDI-TOF-MS, matrix-assisted, laser desorption ionization, time-of-flight mass spectrometry; R_t, retention time

PII S0014-5793(96)00767-3

were prepared with one tissue volume (typically 30 μl for 10 epithelia) ice-cold homogenization buffer (50 mM NH_4HCO_3, 10 mM EGTA, 5 mM dithiothreitol, 1 mM aminoethylbenzenesulfonyl fluoride, 1 mM benzamidine, 5 μg ml^{-1} leupeptin, 5 μg ml^{-1} pepstatin). The supernatant and pellet obtained after ultracentrifugation for 5 min at 2×10^5 Pa ($\approx150000\times g$) in a Beckman Airfuge are referred to as the cytosol and particulate fraction, respectively. For heat treatment, nuclease-treated cytosol was incubated at 90°C for 15 min, chilled on ice, then clarified in the Airfuge as above. Further details were given earlier [15,16].

Mitochondrial inner membranes were prepared from rat liver by Dr. M.P. Murphy of this Department, using sequential treatments of purified mitochondria with the detergents digitonin and Lubrol as described [18]. The liver ATP synthase F_1-α- and F_1-β-subunits were identified by denaturing two-dimensional gel electrophoresis, referring to the published patterns [18,19] and the position of the enamel cell F_1-β-subunit in parallel gels (Fig. 1).

2.2. Gel electrophoresis procedures

SDS-PAGE with the Laemmli discontinuous buffer system, and denaturing two-dimensional gel electrophoresis (both 0.75 mm thick, minigel format), were as described [15].

The ^{45}Ca overlay procedure used to detect calcium-binding proteins following gel electrophoresis and blotting was described before [15]. The overlay solution was 25 mM Tris-HCl, pH 7.2, 100 mM KCl, 1.5 mM $MgCl_2$, containing 5 μM or 50 μM $^{45}CaCl_2$ as specified for detection of high and low affinity calcium-binding proteins, respectively. Calcium-binding proteins were revealed by autoradiography at −80°C, and subsequently stained with Amido black (0.1% in 10% acetic acid, 45% methanol).

Gels and ^{45}Ca overlay autoradiograms were quantified by calibrated imaging densitometry (Model GS670 scanner and Molecular Analyst software, from BioRad), using varied sample loads and autoradiographic exposures to verify linearity, as before [15]. Two dimensional gel spots were quantified manually (fixed area analysis was found to be more accurate than automatic spot detection [16]), using a well resolved and constitutively expressed 32 Da protein (pI 5.0, Fig. 1B) as an internal standard for cross-gel normalization [16]. The F_1-β-subunit concentration was determined by reference to the $calbindin_{28kDa}$ and calreticulin spots, previously quantified in the same set of gels [16], and assuming equal Coomassie blue staining responses for all three proteins.

2.3. Protein microchemistry

In-gel digestion of Coomassie blue-stained two-dimensional gel spots was done as before [15,16] except that a 10-fold lower concentration of the nonionic detergent Thesit (i.e. 0.002% final) was used in the digest and extraction solvents, for compatibility with the MALDI-TOF mass analysis. We have found that higher concentrations of Thesit (>0.08% final in the MALDI sample/matrix mixture) cause a general suppression of peptide ions (M.J. Hubbard, J.C. Kon and D.L. Carne, unpublished data).

Peptides were separated by microbore reverse phase-HPLC on an octadecyl silica column (Aquapore, from Applied Biosystems), then collected manually into siliconized polypropylene microtubes that had been precoated with Thesit (5 μl of 0.002% Thesit) for improved peptide recovery [15]. The peptide fractions (50–100 μl) were stored at −20°C. Automated microsequencing, optimized for high (sub-pmol) sensitivity, was as described [15,16].

For MALDI-TOF-MS, peptide samples (0.5 μl of HPLC fractions) were mixed with an internal standard (0.2 μl of 2 μM substance P, $[M+H]^+=1348.7$) and matrix (0.5 μl of 10 mg ml^{-1} α-cyano-4-hydroxycinnamic acid in 0.1% trifluoroacetic acid, 60% acetonitrile) directly on the stainless steel slide, and left to dry at room temperature. Mass data were collected, at near-threshold laser fluences in the positive ion mode, with a linear instrument (Finnigan Lasermat 2000, from Thermo Bioanalysis).

2.4. Other methods and materials

Protein concentrations were estimated by colorimetric microassay or by Coomassie blue-stained SDS-PAGE as before [15,16]. Paired mean values were compared statistically with Student's *t*-test (two-tailed, homoscedastic). Substance P was from Sigma, α-cyano-4-hydroxycinnamic acid was from Aldrich, aminoethylbenzenesulfonyl fluoride (Pefabloc SC) was from Boehringer Mannheim, and the 10 kDa protein ladder standard for SDS-PAGE was from Life Technologies. Other materials were sourced as described recently [15,16].

3. Results

3.1. Identification of an enamel cell 52 kDa calcium-binding protein as the ATP synthase F_1-β-subunit

Numerous calcium-binding proteins were detected in enamel cell cytosol with the ^{45}Ca-overlay procedure, as reported recently [15,16]. Probing the overlays with a relatively high calcium concentration (50 μM ^{45}Ca) revealed several low affinity calcium-binding proteins including the endoplasmic reticulum residents, calreticulin and endoplasmin (Fig. 1, and [16]).

One unidentified low affinity calcium-binding protein, which migrated on denaturing two-dimensional gels at 52 kDa and pI 5.2 (labelled F_1-β in Fig. 1A), was of particular interest since the corresponding protein spot (Fig. 1B) was both abundant and up-regulated during maturation, suggesting an important function in enamel hypermineralization. Calibrated densitometry of protein spots from parallel Coomassie blue-stained gels (see Section 2.2) indicated that the 52 kDa protein constituted 27 ± 3 μg.mg soluble $protein^{-1}$ ($\pm$SEM, $n=4$) during maturation, and that this level of expression was significantly higher ($152\pm6\%$, $n=4$, $P<0.05$) than that during secretion.

Further experiments (data not shown) revealed that the yield of soluble 52 kDa calcium-binding protein was the same in the presence and absence of a calcium chelator (5 mM EGTA) during tissue disruption, and that the protein was heat labile (i.e. insoluble after heating at 90°C). These properties, also shown by calreticulin and endoplasmin, distinguished the 52 kDa protein from the high affinity calcium-binding proteins, calmodulin and $calbindin_{28kDa}$ [15,16].

To identify the 52 kDa calcium-binding protein, the protein spot (labelled F_1-β in Fig. 1B) was digested with trypsin and subjected to microstructural analysis (Fig. 2). Surprisingly, the initial microsequencing data (peptides 4, 10, 11, 14 and 21; Fig. 2B) indicated identity with the ATP synthase F_1-β-subunit (rat liver cDNA [20,21]), a protein not previously reported to bind calcium specifically. The theoretical mass (51.2 kDa) and charge (pI 4.8) values of the F_1-β-subunit were consistent with those observed experimentally for the 52 kDa calcium-binding protein (Fig. 1).

To examine the possibility that more than one protein was present in the excised gel spots, the primary structural analysis was extended using MALDI-TOF-MS. Mass analysis of 21 chromatographic fractions (Fig. 2A) produced a total of 31 reproducible mass peaks, all of which were assignable to the F1-β-subunit (Fig. 2B) as follows. Most mass peaks corresponded closely (<0.1% mass difference) to the masses of tryptic peptides (17 limit peptides, 4 partials) predicted by direct translation of the F1-β-subunit cDNA sequence [20,21]. The remaining 10 mass peaks differed from predicted F1-β-subunit tryptic peptides by 16 Da or 32 Da, suggesting the possibility of methionine oxidation [22]. Consistent with conversion of methionine to the more hydrophilic methionine sulfoxide, the putative singly oxidized peptides all eluted relatively early from the reverse phase-HPLC column (mean $\Delta R_t=-2.8$min versus the respective unmodified peptides, ranging from approximately −1.5 min for peptides 5, 10, 18 and 19, to −5.8 min for peptide 9) and each had a single

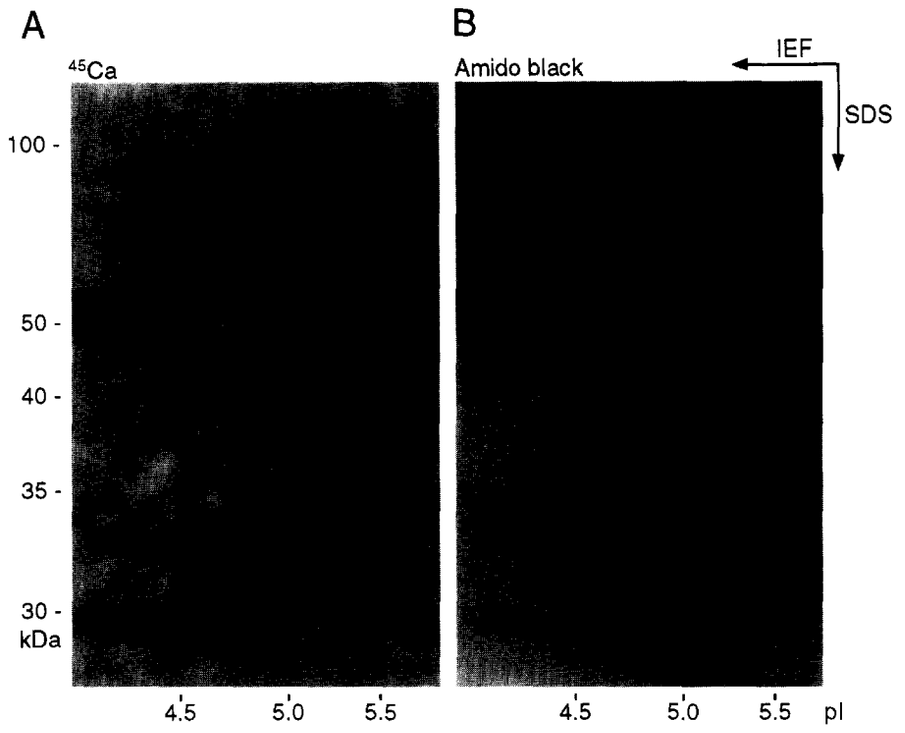

Fig. 1. Detection of an abundant 52 kDa calcium-binding protein in enamel cells. Cytosol from enamel epithelium (60 μg protein, maturation phase) was subjected to denaturing two-dimensional gel electrophoresis (IEF then SDS-PAGE with 14% T, 2.7% C, in the directions shown) and sequential ^{45}Ca overlay analysis with 5 μM then 50 μM $^{45}CaCl_2$ as described in Section 2. (A) 50 μM ^{45}Ca autoradiograph showing the acidic region (pI 4.0–6.0) that contains numerous calcium-binding proteins (redrawn from [16]). The positions of ^{45}Ca spots corresponding to the previously identified proteins endoplasmin (EP), calreticulin (CR), calbindin$_{28kDa}$ (CB28) and actin are indicated, as is the F_1-β-subunit. The mass calibration is imprecise above 50 kDa because of sample compression on this high density gel. (B) Amido black staining of the ^{45}Ca overlay blot shown in A. The spot used as an internal standard for densitometry is indicated (asterisk).

methionine residue. Strikingly one peptide, predicted to contain two methionine residues and identified by partial microsequencing in three separate HPLC fractions (R_t = 33.5 min, 36.0 min and 39.3 min), displayed masses (+32 Da, +16 Da and unmodified, respectively) corresponding to doubly, singly and unoxidized methionines (peptide 14, Fig. 2).

Together, the tryptic peptides identified by microsequencing and mass analysis accounted for 343 residues, constituting 71% of the predicted mature F_1-β-subunit (i.e. 483 residues after removal of the mitochondrial transit sequence [23]). It was concluded that the F_1-β-subunit was the only major constituent of the 52 kDa protein spot.

3.2. *Rat liver mitochondrial F_1-β-subunit binds calcium*

Without a complete primary structural characterization, it remained possible that the calcium-binding properties were a distinct feature of the enamel cell F_1-β protein. Accordingly, mitochondrial inner membranes from rat liver (a classical source of ATP synthase) were subjected to ^{45}Ca overlay analysis.

A single major calcium-binding band was detected, migrating at approximately 52 kDa in one-dimensional separations (data not shown). In two-dimensional overlays, the F_1-β-subunit was again revealed as a calcium-binding protein, whereas the 54 kDa F_1-α-subunit and several other major proteins did not bind ^{45}Ca under these conditions (Fig. 3). This experiment established that calcium binding was specific, and a property of the known F_1-β gene product.

3.3. *Calcium-binding properties of the F_1-β-subunit*

An initial characterization of the F_1-β-subunit calcium-binding properties was undertaken using two-dimensional ^{45}Ca overlays, with near physiological concentrations of Mg^{2+}, K^+ and H^+ (1.5 mM, 100 mM and pH 7.2, respectively). Although this procedure involves denaturing steps, the resultant binding data for a variety of calcium-binding proteins are consistent with the values from conventional nondenaturing equilibrium based methods (e.g. [24–27]).

To assess the affinity for calcium (Fig. 4A), binding data obtained at two calcium concentrations were normalized against those from an internal calmodulin standard, as before [16]. At the higher calcium concentration, the F_1-β-subunit exhibited an approximately 3.5-fold increased calcium binding. Equivalent increases were observed for calreticulin, endoplasmin and protein disulphide isomerase, all of which are low affinity ($K_{app} \approx$ 1–5 mM [24,27,28]) calcium-binding proteins. In contrast, calbindin$_{28kDa}$ showed unaltered binding under these conditions (Fig. 4A), consistent with its known calmodulin-like high affinity ($K_{app} \approx 0.5$ μM [29]) calcium sites. Given the equivalent apparent affinities, it was possible to derive relative calcium binding capacities (Ca^{2+} bound/protein stain unit) for the low affinity proteins (Fig. 4B). The F_1-β-subunit capacity was approximately 42% that of calreticulin, and significantly less than those of endoplasmin and protein disulphide isomerase (both ≈56% of calreticulin). Together, these data characterized the F_1-β-subunit as a (macroscopically) low affinity and moderate capacity calcium-binding protein.

A

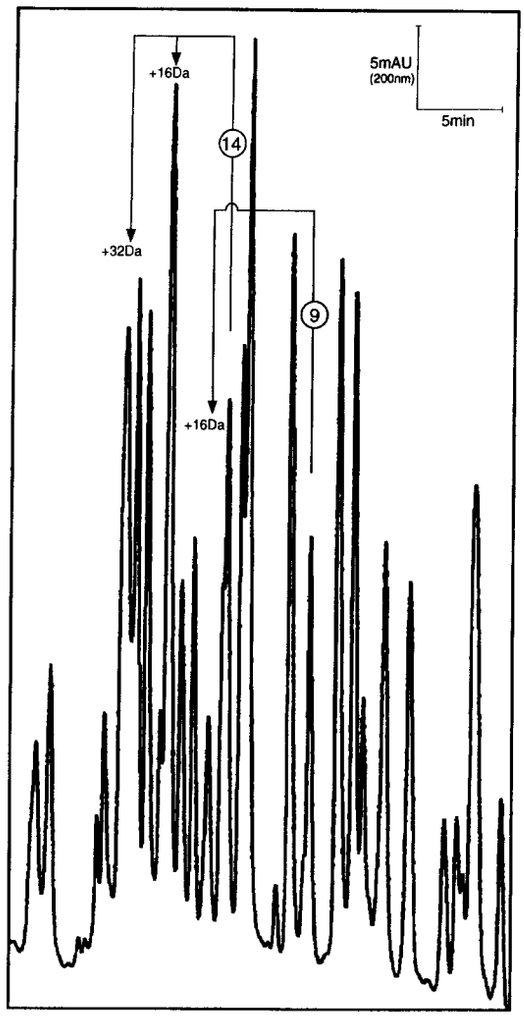

B

Peptide	Sequence Called	Identity to F1-β	Mass Exptal [M+H]+	Known F1-β	F1-β peptide (residues)	Modificn.
1			1652.2	1651.9	49-63	
2			1920.4	1920.3	79-97	
3			1039.7	1039.2	88-97	
4	IMNVIGEPIDER	12/12	1387.0	1386.6	98-109	
			1403.5	1402.6		MetO
5			3027.8	3028.5	116-142	
			3042.9	3044.5		MetO
6			1458.9	1458.8	167-179	
7			1408.3	1407.5	180-193	
8			2319.4	2319.6	194-213	
9			2062.4	2062.3	196-213	
			2079.8	2078.3		MetO
10	VALVYGQMNEPP...	12/12	1603.1	1602.8	219-233	
			1617.2	1618.8		MetO
11	VALTGLTVAE...	10/10	1440.8	1440.7	236-248	
12			1923.4	1923.1	249-264	
13			1437.5	1436.6	265-278	
14	IPSAVGYQP(T)LA...	11/12	2267.0	2267.6	279-299	
			2283.9	2283.6		MetO
			2299.9	2299.6		2 x MetO
15			3844.1	3845.3	305-341	
16			3715.5	3717.1	306-341	
17			1989.0	1989.2	342-360	
18			1816.9	1817.0	361-376	
			1833.7	1833.0		MetO
19			2676.8	2677.0	387-410	
			2692.8	2693.0		MetO
20			2023.4	2024.3	417-434	
			2040.2	2040.3		MetO
21	GFQQILAGDYDHLPEQAFYMVG..	22/22	3337.8	3338.8	444-473	
			3353.7	3354.8		MetO

Fig. 2. Primary structural identification of the enamel cell ATP synthase F_1-β-subunit. Coomassie blue-stained F_1-β spots were excised from 12 two-dimensional minigels (e.g. Fig. 1B), digested in situ with trypsin, and the recovered peptides subjected to reverse phase-HPLC, amino terminal microsequencing and MALDI-TOF-MS as described in Section 2. (A) High sensitivity tryptic peptide map, obtained by gradient elution from a microbore (1 × 100 mm) column equilibrated in 0.1% trifluoroacetic acid (50 μl min^{-1}, 20°C) and monitored at 200 nm. A section of the chromatogram is illustrated, starting at the beginning of the linear acetonitrile gradient (0.8% min^{-1}). The elution positions of peptide 14 (2267 Da), found to contain two (+32 Da, R_t = 33.5 min), one (+16 Da, R_t = 36.0 min) and no oxidized methionines (encircled 14, R_t = 39.3 min), are indicated. The −5.8 min shift in retention of peptide 9 resulting from a single methionine oxidation is also illustrated. Quantitative information cannot be derived from relative peak heights, due to coeluting peptides. (B) Microsequence and mass data, obtained from the tryptic peptides illustrated in A. The extent of identity between the experimentally determined (called) sequence and the indicated residues of the F_1-β-subunit (derived from rat liver cDNA and amino terminal protein sequences [20,21,23]) is represented by the identity ratio, with an ambiguous call (in parentheses; the expected residue is given) excluded. Initial sequencing yields were 5–12 pmol. Experimental masses (*m/z*) for singly protonated species ($[M+H]^+$) are the mean values obtained from at least 3 separate determinations (i.e. different laser aims or samples). Standard errors, which in all cases were ≤ 0.06% of the mean, are omitted for clarity. Modified peptides containing methionine sulfoxide (MetO) are indicated. Eight of the 10 peptide mobility shifts ascribed to methionine oxidation were confirmed by partial microsequencing (data not shown). All assigned peptides were bordered by Arg or Lys, consistent with their tryptic origin.

4. Discussion

This study identified an abundant and developmentally-regulated calcium-binding protein from rat enamel cells as the ATP synthase F_1-β-subunit, a protein not previously recognized to bind calcium specifically. Calcium binding was found to be specific and a general property of this protein, since equivalent behavior was shown by the rat liver F_1-β-subunit but not by the homologous F_1-α-subunit. The F_1-β subunit behaved as a low affinity and moderate capacity calcium-binding protein during comparative ^{45}Ca overlay binding analyses. These findings suggest a new mechanism for the calcium-dependent regulation of ATP synthesis, targeted directly at the catalytic F_1-complex. Importantly, such a mechanism could help coordinate ATP production with the altered demand for ATP-fuelled calcium pump activity that arises from cytosolic calcium variations.

The F_1-β-subunit was characterized as a specific, low affinity and moderate capacity calcium-binding protein, but the physiological significance of calcium binding awaits more detailed investigations. The specificity of calcium binding is supported by three observations. First, calcium binding occurred

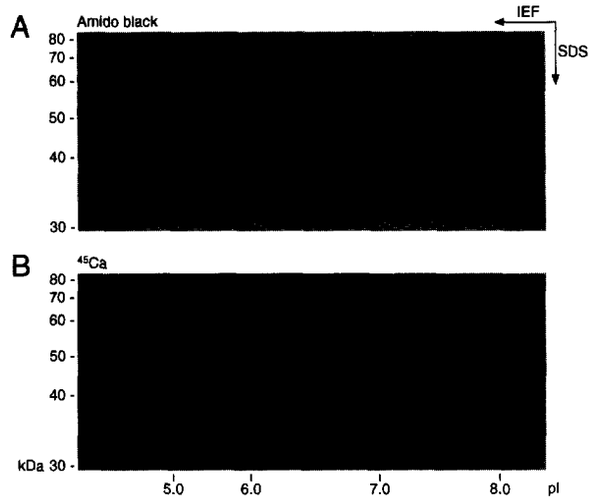

Fig. 3. Calcium binding analysis of rat liver F_1-α- and β-subunits. Mitochondrial inner membranes from rat liver were subjected to denaturing two-dimensional gel electrophoresis (10% T second dimension) and ^{45}Ca overlay analysis, as described in Fig. 1 and Section 2. (A) Protein spots revealed by Amido black staining of the ^{45}Ca overlay blot (30–80 kDa region) shown in B. The F_1-α-subunit and F_1-β-subunit are indicated. (B) 5 μM ^{45}Ca autoradiograph showing detection of the β-subunit but not the α-subunit. The same pattern was observed following reprobing with 50 μM ^{45}Ca (not shown).

at a physiological magnesium concentration (i.e. 300-fold higher than calcium) and ionic strength. This binding behavior is distinct from the broad specificity divalent cation (magnesium) binding characterized previously [11,30,31]. Second, under these conditions, calcium did not bind to the homologous F_1-α-subunit which shares over 20% sequence identity and a similar tertiary structure with the F_1-β-subunit [32]. Since both the F_1-α- and F_1-β-subunits coordinate magnesium at their respective nucleotide-binding sites [32], it can be inferred that the specific calcium sites lie elsewhere on the β-subunit. Third, given mounting evidence that acidic residue clusters can bind calcium specifically [27,33,34], several candidate calcium-binding sites are evident in the globally acidic (pI 4.8) F_1-β-subunit. Most notable is a highly conserved superficial loop of the F_1-β-subunit that contains the acidic sequence DELSEED, is known to bind cationic inhibitors, and is not mirrored in the basic (theoretical pI 8.8) F_1-α-subunit [19,32,35]. Consistent with calcium binding to acidic residue clusters, the F_1-β-subunit exhibited the same apparent affinity (Fig. 4A) as three calcium-binding proteins enriched with such sites [34]. However, it should be recognized that at the coarse level of analysis done here, binding to a small number of high affinity sites would be obscured. Indeed, both calreticulin and endoplasmin contain one or more high affinity calcium-binding sites, besides the predominant low affinity sites [27,36,37]. The data in Fig. 4B suggest that the maximum capacity (B_{max}) of the F_1-β-subunit is in the order

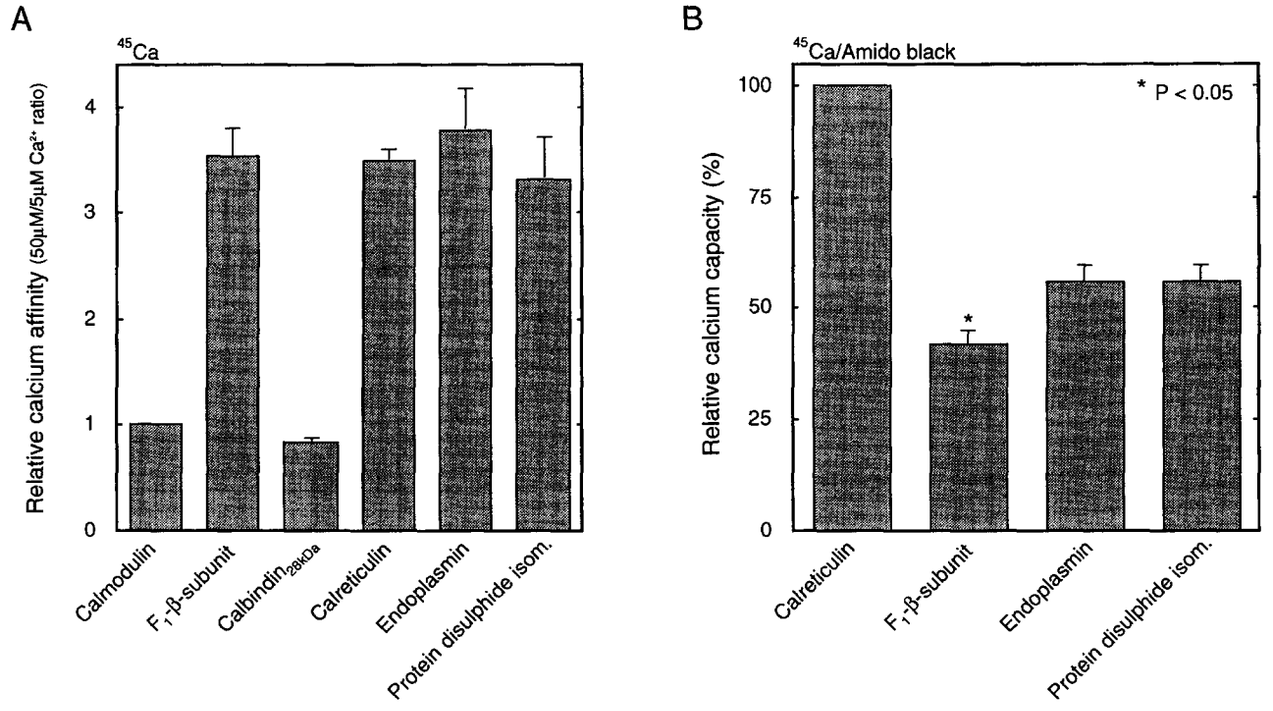

Fig. 4. Calcium binding properties of the F_1-β-subunit. Enamel cell cytosol was subjected to two-dimensional ^{45}Ca overlay analysis and developed successively with 5 μM then 50 μM $^{45}CaCl_2$, as in Fig. 1. The data (mean ± SEM) are from three separate experiments with two cytosol preparations (each from ≥ 20 epithelia). (A) Relative calcium affinities for the F_1-β-subunit and the indicated known calcium-binding proteins, where a higher value corresponds to lower affinity. Calcium-binding protein spots were quantitated by imaging densitometry of autoradiographs made in the linear range for both calcium concentrations, and the resultant ratio data (i.e. digital volumes of 50 μM vs. 5 μM ^{45}Ca spots) were normalized against those of an internal calmodulin standard run in the mass calibration lane. Protein disulphide isomerase (the major 55 kDa, pI 5.3 spot above the F_1-β-subunit in Fig. 1) was identified by primary structural analysis (unpublished data). (B) Relative calcium capacities for the F_1-β-subunit and the other low affinity proteins identified in A. For each spot, the 50 μM ^{45}Ca binding value was divided by the Amido black staining intensity and then normalized as a percentage of calreticulin, to enable comparison between data sets. $^*P < 0.05$ for F_1-β-subunit vs. endoplasmin and protein disulphide isomerase.

of 7–18 mol Ca^{2+}/mol, when normalized against the published capacities for 46 kDa calreticulin (20–50 mol Ca^{2+}/mol [27]; note that calreticulin has an anomalous M_r on SDS-PAGE). The same comparison (Fig. 4B) gives values of 6–14 mol Ca^{2+}/mol for 91 kDa endoplasmin (vs. 10–25 mol Ca^{2+}/mol [24,27,36]) and 9–23 mol Ca^{2+}/mol for 55 kDa protein disulphide isomerase (vs. 19–23 mol Ca^{2+}/mol [28]), assuming equal calcium affinities and Amido black staining responses for all proteins.

Calcium binding is probably a general feature of the highly conserved F_1-β-subunit [19], at least from mitochondrial and chloroplast ATP synthases. Our initial ^{45}Ca overlay analysis of mitochondrial inner membranes from several rat and bovine tissues has revealed an appropriate 52 kDa calcium-binding band (P.G. Howell, M.P. Murphy and M.J. Hubbard, unpublished), and weak calcium binding was observed in the α/β-subunit region of chloroplast ATP synthase [14]. Such conservation would suggest an important function, but the physiological significance of calcium binding must await more detailed investigations with a nondenaturing assay. It will be important to characterize binding to the native F_1-β-subunit both in isolation and when part of the holoenzyme. Only then will it be possible to evaluate possible roles of calcium binding (e.g. signalling trigger, ligand binding, structural) in the context of physiological intramitochondrial calcium concentrations. It is noteworthy that a direct calcium binding mechanism was earlier discounted, since calcium activation of ATP synthase persisted following sample dilution [6]. Perhaps assembly of the native holoenzyme, or association with an interacting protein (e.g. CaBI), leads to high affinity calcium binding and a persistent active state. Mechanistic uncertainties aside, identification of the catalytic F_1-β-subunit as a calcium-binding protein introduces new means by which ATP synthase might be calcium regulated.

The observed up-regulation and abundance of the F_1-β-subunit (2.7% of soluble protein) during enamel maturation is consistent with other evidence indicating that the calcium homeostatic burden [15,16], calcium transport [38] and expression levels of the plasma membrane calcium pump [39] are maximal at this time. However, the particular roles (e.g. ATP synthesis, calcium buffering) of mitochondria in enamel cell calcium homeostasis remain to be established. The 1.5-fold postsecretory up-regulation of the F_1-β-subunit is somewhat less than that seen for calreticulin and endoplasmin (1.8- and 2.1-fold, respectively [16]), but equivalent to the increased mitochondrial volume determined by stereology [40]. Appearance of the F_1-β-subunit in enamel cell cytosol probably reflects the mode of tissue disruption used (i.e. vigorous homogenization in the absence of osmotic stabilizers), since an equivalent preparation from liver contained substantial soluble F_1-β-subunit (unpublished data).

Primary structural identification of the enamel cell F_1-β-subunit was complicated by heterogeneity arising from partial oxidation of methionines (Fig. 2). The heterogeneity was evident during both the HPLC and the mass analyses, compromising high sensitivity peptide recovery and mass database searching, respectively. We consider it probable that the methionine oxidations occurred in vitro, as concluded for other proteins analyzed this way (e.g. [22,41]), since all (detected) methionine-containing peptides were affected and a co-analyzed protein spot was similarly oxidized. In contrast, physiologically regulated methionine sulfoxide formation is a highly specific phenomenon [42].

In conclusion, recognition that the catalytic F_1-β-subunit binds calcium introduces interesting new possibilities for calcium-dependent regulation of ATP synthesis. The challenge now remains to uncover the mechanisms involved and to establish their physiological significance.

Acknowledgements: We thank Michael Murphy for guidance with mitochondrial matters and for providing the mitochondrial inner membranes, Diana Carne for assistance with protein microchemistry, and our other colleagues who gave constructive comments and support. This work and purchase of the mass spectrometer were funded by grants from the Health Research Council of New Zealand, New Zealand Lottery Health Research and the University of Otago.

References

[1] Carafoli, E. (1987) Annu. Rev. Biochem. 56, 395–433.
[2] Gunter, T.E., Gunter, K.K., Sheu, S.S. and Gavin, C.E. (1994) Am. J. Physiol. 267, C313–C339.
[3] Jouaville, L.S., Ichas, F., Holmuhavedov, E.L., Camacho, P. and Leichleiter, J.D. (1995) Nature 377, 438–441.
[4] Herrington, J., Park, Y.B., Babcock, D.F. and Hille, B. (1996) Neuron 16, 219–228.
[5] Crompton, M. (1990) in: Intracellular Calcium Regulation (Bronner, F., Ed.), pp. 181–209, Alan R. Liss, New York.
[6] Harris, D.A. and Das, A.M. (1991) Biochem. J. 280, 561–573.
[7] McCormack, J.G. and Denton, R.M. (1994) News Physiol. Sci. 9, 71–76.
[8] MacDonald, M.J. and Brown, L.J. (1996) Arch. Biochem. Biophys. 326, 79–84.
[9] Penefsky, H.S. and Cross, R.L. (1991) Adv. Enzymol. 64, 173–214.
[10] Pedersen, P.L. and Amzel, L.M. (1993) J. Biol. Chem. 268, 9937–9940.
[11] Pedersen, P.L., Williams, N. and Hullihen, J. (1987) Biochemistry 26, 8631–8637.
[12] Yamada, E.W. and Huzel, N.J. (1985) Cell Calcium 6, 469–479.
[13] Yamada, E.W. and Huzel, N.J. (1989) Biochemistry 28, 9714–9718.
[14] Zakharov, S.D., Ewy, R.G. and Dilley, R.A. (1995) Protoplasma 184, 42–49.
[15] Hubbard, M.J. (1995) Eur. J. Biochem. 230, 68–79.
[16] Hubbard, M.J. (1996) Eur. J. Biochem. 239, 611–623.
[17] Hubbard, M.J. and McHugh, N.J. (1995) FEBS Lett. 374, 333–337.
[18] Henslee, J.G. and Srere, P.A. (1979) J. Biol. Chem. 254, 5488–5497.
[19] Walker, J.E., Fearnley, I.M., Gay, N.J., Gibson, B.W., Northrop, F.D., Powell, S.J., Runswick, M.J., Saraste, M. and Tybulewicz, V.L.J. (1985) J. Mol. Biol. 184, 677–701.
[20] Garboczi, D.N., Fox, A.H., Gerring, S.L. and Pedersen, P.L. (1988) Biochemistry 27, 553–560.
[21] Boulet, D., Poirier, J. and Cote, C. (1989) Biochem. Biophys. Res. Commun. 159, 1184–1190.
[22] Patterson, S.D. (1994) Anal. Biochem. 221, 1–15.
[23] Cretin, F., Baggetto, L.G., Denoroy, L. and Godinot, C. (1989) Biochem. Biophys. Res. Commun. 164, 1165–1169.
[24] Macer, D.R.J. and Koch, G.L.E. (1988) J. Cell Sci. 91, 61–70.
[25] Leiser, M. and Sherwood, L.M. (1989) J. Biol. Chem. 264, 2792–2800.
[26] Racchetti, G., Papazafiri, P., Volpe, P. and Meldolesi, J. (1994) Biochem. Biophys. Res. Commun. 203, 828–833.
[27] Michalak, M., Milner, R.E., Burns, K. and Opas, M. (1992) Biochem. J. 285, 681–692.
[28] Lebeche, D., Lucero, H.A. and Kaminer, B. (1994) Biochem. Biophys. Res. Commun. 202, 556–561.
[29] Cheung, W.T., Richards, D.E. and Rogers, J.H. (1993) Eur. J. Biochem. 215, 401–410.
[30] Smith, R.A., Latchney, L.R. and Senior, A.E. (1985) Biochemistry 24, 4490–4494.

[31] Futai, M., Shimomura, S. and Maeda, M. (1987) Arch. Biochem. Biophys. 254, 313–318.
[32] Abrahams, J.P., Leslie, A.G.W., Lutter, R. and Walker, J.E. (1994) Nature 370, 621–628.
[33] Rao, Z., Handford, P., Mayhew, M., Knott, V., Brownlee, G.G. and Stuart, D. (1995) Cell 82, 131–141.
[34] Lucero, H.A., Lebeche, D. and Kaminer, B. (1994) J. Biol. Chem. 269, 23112–23119.
[35] Bullough, D.A., Ceccarelli, E.A., Roise, D. and Allison, W.S. (1989) Biochim. Biophys. Acta 975, 377–383.
[36] Van, P.N., Peter, F. and Soling, H.D. (1989) J. Biol. Chem. 264, 17494–17501.
[37] Csermely, P., Miyata, Y., Schnaider, T. and Yahara, I. (1995) J. Biol. Chem. 270, 6381–6388.
[38] Takano, Y., Crenshaw, M.A. and Bawden, J.W. (1992) Arch. Oral Biol. 37, 377–383.
[39] Borke, J.L., Zaki, A.E., Eisenmann, D.R., Ashrafi, S.H., Ashrafi, S.S. and Penniston, J.T. (1993) J. Histochem. Cytochem. 41, 175–181.
[40] Smith, C.E. (1984) INSERM 125, 273–282.
[41] Sutton, C.W., Pemberton, K.S., Cottrell, J.S., Corbett, J.M., Wheeler, C.H., Dunn, M.J. and Pappin, D.J. (1995) Electrophoresis 16, 308–316.
[42] Brot, N. and Weissbach, H. (1983) Arch. Biochem. Biophys. 223, 271–281.